

Macroporous nanowire nanoelectronic scaffolds for synthetic tissues

Bozhi Tian^{1,2,3†}, Jia Liu^{1†}, Tal Dvir^{2,4†}, Lihua Jin⁵, Jonathan H. Tsui², Quan Qing¹, Zhigang Suo⁵, Robert Langer^{3,4}, Daniel S. Kohane^{2*} and Charles M. Lieber^{1,5*}

¹Department of Chemistry and Chemical Biology, Harvard University, Cambridge, Massachusetts 02138, USA,

²Department of Anesthesiology, Division of Critical Care Medicine, Children's Hospital Boston, Harvard Medical School, Boston, Massachusetts 02115, USA,

³David H. Koch Institute for Integrative Cancer Research, Massachusetts Institute of Technology, Cambridge, Massachusetts 02139, USA,

⁴Department of Chemical Engineering, Massachusetts Institute of Technology, Cambridge, Massachusetts 02139, USA,

⁵School of Engineering and Applied Sciences, Harvard University, Cambridge, Massachusetts 02138, USA,

[†]These authors have contributed equally to this manuscript.

*email: Daniel.Kohane@childrens.harvard.edu; cml@cmliris.harvard.edu

Materials and Methods

Nanowire Synthesis. Single-crystalline nanowires were synthesized using the Au nanocluster-catalyzed vapor-liquid-solid growth mechanism in a home-built chemical vapor (CVD) deposition system described previously^{S1-S3}. Au nanoclusters (Ted Pella Inc., Redding, CA) with either 20 or 80 nm diameters were dispersed on the oxide surface of silicon/SiO₂ substrates (600 nm oxide) and placed in the central region of a quartz tube CVD reactor system. Uniform 20 nm *p*-type silicon nanowires, which were used for mesh-like NWFET scaffolds, were synthesized using reported methods^{S1,S2}. In a typical synthesis, the total pressure was 40 torr and the flow rates of SiH₄, B₂H₆ (100 ppm in H₂) and H₂ were 2, 2.5 and 60 standard cubic centimetres per minute (SCCM), respectively. The silicon-boron feed-in ratio was 4000:1, and the total nanowire growth time was 30 min. Kinked 80 nm diameter silicon nanowires, which were used for the reticular NWFET scaffolds, were synthesized with a $n^+(arm)-n(device)-n^+(arm)$ dopant profile as described recently^{S3}. In a typical synthesis, the total pressure was 40 torr and the flow rates of SiH₄, PH₃ (1000 ppm in H₂) and H₂ were 1, 5/0.1 and 60 sccm, respectively. Kinks were introduced by evacuation of the reactor ($\sim 3 \times 10^{-3}$ torr) for 15 s, and the silicon–phosphorus feed-in ratios were 200:1 and 10,000:1 for the n^+ - and *n*-type segments, respectively. The n^+ -type arms were grown for 12–15 min, and the *n*-type active device channel segment was grown for 30 s immediately following the evacuation step used to introduce a kink.

Free-standing nanoES. The free-standing nanoES were fabricated on the oxide or nitride surfaces of silicon substrates (600nm SiO₂ or 100 SiO₂/200 Si₃N₄, *n*-type 0.005 V·cm, Nova Electronic Materials, Flower Mound, TX) prior to relief from the substrate. Two basic types of nanoES, termed reticular and mesh nanoES, were prepared. Key steps used in the fabrication of the reticular nanoES (Fig. S1) were as follows: (1) Electron beam lithography (EBL) was used to pattern a double layer resist consisting of 500–600 nm of methyl methacrylate (MMA, MicroChem Corp., Newton, MA) and 100–200 nm of poly(methyl methacrylate) (PMMA, MicroChem Corp., Newton, MA), on which 100 nm nickel metal was deposited (Fig. S1a,b), where the nickel served as the final relief layer for the free-standing scaffolds. (2) A 300–500 nm layer of SU-8 photoresist (2000.5, MicroChem Corp., Newton, MA) was deposited over the entire chip (Fig. S1c) followed by pre-baking at 65 °C and 95 °C for 2 and 4 min, respectively,

then (3) the $n^+ - n - n^+$ kinked nanowires were dispersed on the SU-8 layer by dropping an isopropanol solution of the nanowires onto the SU-8 layer and allowing the solution to evaporate (Fig. S1d). (4) The kinked nanowire positions were located relative to a standard marker pattern^{S4} using an optical microscope (Olympus BX51) in dark-field mode, and then IGOR Pro (WaveMetrics) and DesignCAD were used to design the lithography patterns. EBL was then used to pattern the overall SU-8 scaffold structure including a ring structure underneath the selected kink nanowire. After post-baking (65 °C and 95 °C for 2 and 4 min, respectively), the SU-8 developer (MicroChem Corp., Newton, MA) was used to develop the SU-8 pattern. The areas exposed to electron beam became fully polymerized and insoluble in SU-8 developer, which ‘glued’ the selected nanowires in place. The rest SU-8 areas including nanowires on their surfaces were removed by SU-8 developer. After curing (180 °C, 20 min), patterned SU-8 ribbons as flexible structural support for metal interconnects and nanowires were generated (Fig. S1e). (5) The silicon substrate was then coated with MMA and PMMA double layer resist, the resist was patterned over a subset of SU-8 ribbons for defining the metal interconnects, and then nonsymmetrical Cr/Pd/Cr (1.5/50-80/50-80 nm) metals were sequentially deposited followed by metal lift-off in acetone to form the nanowire interconnects (Fig. S1f). The nonsymmetrical Cr/Pd/Cr layer structure yields a built-in stress^{S4}, which drove 3D self-organization when the structure was relieved from the substrate. (6) The silicon substrate was then coated with a uniform 300-400 nm layer of SU-8, and EBL of SU-8 followed by curing (180 °C, 20 min) was used to define the SU-8 passivation layer over the deposited metal interconnects (Fig. S1g). (7) The reticular nanoES, including the interconnected kinked NWFET devices, was released from the substrate by etching of the nickel layer (Nickel Etchant TFB, Transene Company Inc., Danvers, MA) for 60-120 min at 25 °C (Fig. S1h). Last, the free-standing nanoES were dried using a critical point dryer (Autosamdri 815 Series A, Tousimis, Rockville, MD) and stored in the dry state prior to use in tissue culture. Here, self-organization produced random reticular scaffolds, but we note that mechanics models and simulations (*e.g.* finite element method)^{S5} could be used to design and realize regular three-dimensional (3D) open framework constructs using the same general approach (Fig. S4).

A similar approach was used in the fabrication of the mesh nanoES, where the key steps (Fig. S2) were as follows: (1) Photolithography and metal deposition (100 nm, nickel) were used to define a relief layer for the free-standing scaffold (Figs. S2a,b). (2) A layer of SU-8 photoresist

(300–2000 nm, 2000.5 or 2002, MicroChem Corp., Newton, MA) was deposited over the entire chip, and photolithography was used to pattern the bottom SU-8 mesh structure (Fig. S2c), which was then cured (180 °C, 20 min). (3) A second 300–500 nm thick layer of SU-8 was deposited over the entire chip, and prebaked at 65 °C and 95 °C for 2 and 4 min, respectively (Fig. S2d). (4) Then *p*-type silicon nanowires were deposited from isopropanol solution and aligned by nitrogen blow-drying (Fig. S2e). (5) Photolithography and subsequent curing (180 °C, 20 min) was used to define the nanowire patterns across the mesh structure. Similar to the fabrication of reticular nanoES, the nanowires on areas without exposure to ultraviolet light are washed away during SU-8 development. (Fig. S2f). (6) The substrate was coated with S1805 and LOR 3A (MicroChem Corp., Newton, MA) double layer resist and patterned by photolithography. Symmetrical Cr/Pd/Cr (1.5/50–100/1.5 nm) metals were sequentially deposited followed by metal lift-off in Remover PG (MicroChem Corp., Newton, MA) to define the minimally stressed nanowire interconnects (Fig. S2g). (7) The substrate was coated with a uniform layer of SU-8, and photolithography followed by curing (180 °C, 20 min) was used to define a passivation layer over the deposited metal interconnects (Fig. S2h). (8) The mesh-like nanoES was released from the substrate by etching the nickel layer (Nickel Etchant TFB, Transene Company Inc., Danvers, MA) for 6 h at 25 °C (Fig. S2h). The mesh-like scaffold adhered weakly to the substrate upon drying in air, and could be readily suspended as a free-standing scaffold upon immersion in water/cell culture medium. Scanning electron microscopy (SEM, Zeiss Ultra55/Supra55VP field-emission SEMs) was used to characterize both types of fabricated scaffold structures.

NanoES/collagen(MatrigelTM) hybrid matrix. Prior to gel casting, collagen type-I (Sigma-Aldrich Corp., St. Louis, MO) was diluted (1:2 ~ 1:5) with culture media or phosphate buffered saline solution (PBS) and the pH was adjusted to ~ 7.4. MatrigelTM (BD Bioscience, Bedford, MA) was used as received or diluted (1:2 ~ 1:5). Briefly, 50 ~ 2000 µL collagen or Matrigel solution was placed using a pipette (Eppendorf Research plus) onto the edge of (reticular nanoES) or directly above (mesh nanoES) the nanoES scaffolds, and at ~ 4 °C. The solutions were allowed to form gels around nanoES under 37 °C, 5 % CO₂ condition for at least 20 min. For visualization of collagen fibers, fluorescein isothiocyanate labelled collagen type-I (Sigma-Aldrich Corp., St. Louis, MO) was used.

NanoES/alginate hybrid scaffold. The 3D nanoES/alginate scaffolds were prepared from pharmaceutical-grade alginate, Protanal LF5/60 (FMC Biopolymers), which has a high guluronic acid (G) content (65%). Briefly, (1) preparation of sodium alginate stock solutions at concentrations of 1% (w/v); (2) partially crosslinking the alginate solution by adding calcium gluconate; (3) drop casting partially crosslinked alginate onto loosely folded mesh nanoES, followed by additional shaping and placement of nanoES inside the alginate gel with a glass rod; (4) freezing the nanoES/alginate gel in a homogeneous, cold (-20°C) environment; and (5) lyophilization to produce a sponge like scaffold ($5\sim 15\text{ mm} \times 2\sim 10\text{ mm}$, $d \times h$).

NanoES/PLGA hybrid scaffold. Poly(lactic-co-glycolic acid) (PLGA) electrospun fibers were used as a secondary scaffold in several experiments. The PLGA fibers were prepared based on reported procedures^{S6} as follows. PLGA (90/10 glycolide/L-lactide, inherent viscosity 1.71 dL/g in HFIP at 25°C , Purac Biomaterials Inc.) was dissolved in 1,1,1,3,3,3-hexafluoro-2-propanol (HFIP, Sigma-Aldrich Corp., St. Louis, MO) at a 10 wt% concentration until a clear and homogenous solution was obtained. A syringe pump (Harvard Apparatus, Holliston, MA) was used to deliver the polymer solution through a stainless steel capillary at a rate of 3 mL/hr. A high voltage power supply (Gamma High Voltage Research, Ormond Beach, FL) was used to apply a 25 kV potential between the capillary tip and a grounded stainless steel plate 50 cm away. Fibers were collected for 2-5 minutes before being put aside at room temperature for 72 hours to allow residual solvent evaporate. To prepare hybrid scaffolds, a sheet of PLGA fibers with diameters of $\sim 1\text{--}3\text{ }\mu\text{m}$ was deposited on both sides of the mesh nanoES. The hybrid scaffold can be folded to increase thickness.

Scaffold mechanical properties. The effective bending stiffness per unit width of the mesh scaffold, \overline{D} , can be estimated by^{S5}

$$\overline{D} = \alpha_s D_s + \alpha_m D_m$$

where α_s and α_m are the area fraction of the single-layer polymer (SU-8) ribbon (without metal layer and top polymer passivation layer) and three-layer ribbon (bottom polymer layer, metal

layer and top passivation layer) in the whole mesh structure. $D_s = E_s h^3 / 12$ is the bending stiffness per unit width of the single-layer polymer, where $E_s = 2\text{GPa}$ and h are the modulus and thickness of the SU-8. D_m is the bending stiffness per unit width of a three-layer structure, which can be calculated by^{S7}

$$D_m = \frac{E_m b_m h_m^3}{12b} + \frac{E_s}{b} \left(\frac{(b - b_m)(2h + h_m)^3}{12} + \frac{1}{6} b_m h^3 + 2b_m h \left(\frac{h}{2} + \frac{h_m}{2} \right)^2 \right)$$

where $E_m = 121\text{GPa}$ and h_m are the modulus and thickness of the palladium, b is the width of the single-layer ribbon and the total width of the three-layer ribbon, b_m is the width of the palladium layer. In addition, the chromium layers are so thin (1.5 nm) that their contribution to the bending stiffness is negligible. When $h_m = 75\text{nm}$, $h = 0.5\mu\text{m}$, $b = 10\mu\text{m}$, $b_m = 5\mu\text{m}$, $\alpha_s = 2.51\%$ and $\alpha_m = 3.57\%$, we can calculate $\bar{D} = 0.006\text{nN} \cdot \text{m}$. When $h_m = 75\text{nm}$, $h = 2\mu\text{m}$, $b = 40\mu\text{m}$, $b_m = 20\mu\text{m}$, $\alpha_s = 10.06\%$ and $\alpha_m = 13.31\%$, we can calculate $\bar{D} = 1.312\text{nN} \cdot \text{m}$.

To calculate the strain in tubular constructs, we used the equation $\varepsilon = y/R$, where y is the distance from the neutral plane, and R is the radius of curvature^{S7}. For the symmetric mesh scaffold, since the neutral plane is the middle plane, the maximum strains of metal and SU-8 appear at $y = h_m/2$ and $y = h_m/2 + h$, respectively. When $h_m = 75\text{nm}$, $h = 2\mu\text{m}$, $R = 0.75\text{mm}$, the maximum strains of metal and SU-8 are 0.005% and 0.272%, respectively.

Scaffold structural simulation. The self-organization of the mesh structure due to residual stress was simulated by the commercial finite element software ABAQUS. Both the SU-8 ribbons and the SU-8 / metal ribbons were modeled as beam elements. The cross-sectional property of the SU-8 / metal ribbons was defined by the appropriate meshed beam cross-section, while the cross-sectional property of the SU-8 ribbons was set by defining the relevant rectangular profile. The equivalent bending moment on SU-8 / metal ribbons was calculated using the residual stress measured by MET-1 FLX-2320-S thin film stress measurement system, which were 1.35 and 0.12 GPa for Cr (50 nm) and Pd (75 nm), respectively.

Cell culture.

A. Neuron culture: Device chips were cleaned by oxygen plasma (50 sccm of O₂, 50 w, 0.5 Torr, 1 min), and fixed onto a temperature controlled chamber (Warner Instruments, Hamden, CT) with double-sided tape (Fig. S5a). A 1 mm thick polydimethylsiloxane (PDMS) membrane (Sylgard 184, Dow Corning, Inc., Midland, MI) with 0.25 cm² open area in the center was cut, autoclaved and placed over the device area, followed by wire-bonding of individual devices (Fig. S5b). An autoclaved glass ring (ALA Scientific Instruments, Farmingdale, NY) was placed over this PDMS chamber and fixed with Kwik-Sil (World Precision Instruments, Inc., Sarasota, FL) silicone elastomer (Fig. S5c). The whole chip was sterilized by UV illumination and 75% ethanol soak (20 min each). An aqueous polylysine solution (0.5-1.0 mg/ml, MW 70,000 – 150,000, Sigma-Aldrich) was then introduced into the chamber and incubated overnight at 37 °C, the polylysine solution was removed, and the chamber rinsed 3 times each with 1X phosphate buffered saline (PBS) solution and NeuroPure Plating Medium (Genlantis, San Diego, CA). Finally, the chamber was filled with NeuroPure Plating Medium or culture medium and conditioned in the incubator for 1 day. Hippocampal neurons (Gelantis, CA) were prepared using a standard protocol^{S8}. In brief, 5 mg of NeuroPapain Enzyme (Gelantis, CA) was added to 1.5 ml of NeuroPrep Medium (Gelantis, San Diego, CA). The solution was kept at 37 °C for 15 min, and sterilized with a 0.2 µm syringe filter (Pall Corporation, MI). Day 18 embryonic Sprague/Dawley rat hippocampal tissue with shipping medium (E18 Primary Rat Hippocampal Cells, Gelantis, San Diego, CA) was spun down at 200 g for 1 min. The shipping medium was exchanged for NeuroPapain Enzyme medium. A tube containing tissue and the digestion medium was kept at 30 °C for 30 min and manually swirled every 2 min, the cells were spun down at 200 g for 1 min, the NeuroPapain medium was removed, and 1 ml of shipping medium was added. After trituration, cells were isolated by centrifugation at 200 g for 1 min, then re-suspended in 5-10 mg/ml MatrigelTM (BD Bioscience, Bedford, MA) at 4 °C. The cell/MatrigelTM mixture was plated on the reticular nanoES in the opening in the PDMS membrane at a density of 2 – 4 million cells /ml and a total gel thickness of ~0.5-1 mm. The MatrigelTM matrix was allowed to gel at 37 °C for 20 min, then 1.5 ml of NeuroPure Plating Medium was added, and the entire assembly was placed in the incubator. After 1 day, the plating medium was changed to NeurobasalTM medium (Invitrogen, Grand Island, NY) supplemented with B27 (B27 Serum-Free Supplement, Invitrogen, Grand Island, NY), GlutamaxTM (Invitrogen, Grand Island, NY) and 0.1% Gentamicin reagent solution (Invitrogen, Grand Island, NY)^{S9}. 3D

neuron cultures were maintained at 37 °C with 5% CO₂ for 7–21 days, with medium changed every 4–6 days. For cultures lasting longer than 7 days, gas-permeable/water-impermeable membrane covers (ALA MEA-MEM-PL, ALA Scientific Instruments, Farmingdale, NY) were used to avoid evaporation while allowing for diffusion of gases (Fig. S5d).

B. Cardiomyocyte culture. Hybrid scaffolds (Fig. S7b) consisting of the mesh nanoES (Figs. S7a, S7g) sandwiched between two electrospun PLGA fiber layers (1–3 µm diameter; 10–20 µm thick for individual layer) were used in all experiments. The bottom PLGA layer was made either by inserting an existing layer underneath the mesh-like scaffold or by directly electrospinning on the nanoES. The top PLGA layer was made by direct electrospinning on the nanoES.

The device chip was wire-bonded (Figs. S7c, S7h), and assembled with a modified polystyrene petri-dish (VWR Inc.) using Kwik-Sil (World Precision Instruments, Inc) silicone elastomer glue (Fig. S7d). The device chamber was cleaned by oxygen plasma (50 sccm of O₂, 50 w, 0.5 Torr, 1 min), followed by sterilization with UV-light illumination for 1 h and soaking in 70 % ethanol solution for 0.5 h. The hybrid scaffolds were coated with fibronectin/gelatin solution overnight prior to cell seeding. The fibronectin/gelatin solution was prepared by adding 0.1 g Bacto-Gelatin (Fisher Scientific, DF0143-17-9) to 500 mL distilled water in a glass bottle and autoclaving. The gelatin dissolved during the autoclaving step to yield a final concentration of gelatin of 0.02 %. One ml Fibronectin (Sigma, F-1141) was diluted in 199 ml of 0.02 % gelatin.

Cardiac cells were isolated from intact ventricles of 1 to 3-day-old neonatal Sprague/Dawley rats using 3–4 cycles (30 min each) of enzyme digestion using collagenase type II and pancreatin as described elsewhere^{S10}. The cells were suspended in culture medium, composed of Medium-199 (Invitrogen, Grand Island, NY) supplemented with 0.6 mM CuSO₄·5H₂O, 0.5 mM ZnSO₄·7H₂O, 1.5 mM vitamin B12, 500 U ml⁻¹ penicillin, 100 mg ml⁻¹ streptomycin and 5 vol.% fetal calf serum (FCS)^{S10}. The cardiac cells were finally seeded with 5–10 mg/ml MatrigelTM onto fibronectin/gelatin coated PLGA/mesh nanoES at an initial cell density of 3–6 × 10⁷ cm⁻² (Fig. S7e). After 1–2 days, the cell-seeded nanoES was manually folded into a construct, and was maintained at 37 °C with 5% CO₂ for an additional 3–8 days (Fig. S7f), with medium changes

every 2-3 days. All animal procedures conformed to US National Institutes of Health guidelines and were approved by Harvard University's Animal Care and Use Committee.

C. Vascular construct. Synthetic vascular constructs were produced in a manner similar to the sheet-based tissue engineering approach described previously^{S11} (Fig. S12). First, the mesh nanoES were coated with gelatin/fibronectin solution overnight (Figs. S12a-c). Second, human aortic smooth muscle cells (HASMC, Invitrogen, Grand Island, NY) were seeded at a density of $1 \times 10^4 \text{ cm}^{-2}$ on the gelatin/fibronectin-coated devices and cultured in Medium 231 (Invitrogen, Grand Island, NY) supplemented with smooth muscle growth supplement (SMGS, Invitrogen) (Fig. S12d). Sodium L-ascorbate ($50 \mu\text{g} \cdot \text{mL}^{-1}$, Sigma) was added to the culture medium to stimulate extracellular matrix (ECM) synthesis^{S11}. HASMCs were maintained at 37°C with 5% CO_2 until their secreted ECM proteins formed an cohesive tissue sheet (7-14 days)^{S11} that can be easily peeled off from the silicon substrate. The cell-coated mesh nanoES was then gently lifted from the SiO_2 substrate using fine forceps, rolled onto a polystyrene or glass tubular support 1.5 mm in diameter, then maintained in culture Medium 231 supplemented with SMGS and $50 \mu\text{g} \cdot \text{mL}^{-1}$ sodium L-ascorbate for at least another 2 weeks for maturation of the vascular structure (Fig. S12e).

0.5-2 h prior to pH sensing experiments, the temporary tubular support was removed, and segments of polystyrene tubing (the inner tubing in Fig. 6f, inset) were connected to the open ends of the vascular construct (Fig. S12f), and a PDMS fluidic chamber with input/output tubing and Ag/AgCl electrodes (Fig. 6f, inset) was sealed with the silicon substrate and the vascular construct using silicone elastomer glue (Kwik-Sil, World Precision Instruments, Inc) as shown in Fig. S12h. Fresh medium was delivered to the vascular construct through both inner and outer tubing. The pH of the solution delivered through the outer tubing was varied during the experiment.

Immunochemical staining. Cells were fixed with 4% paraformaldehyde (Electron Microscope Sciences, Hatfield, PA) in PBS for 15-30 min, followed by 2-3 washes with ice-cold PBS. Cells were pre-blocked and permeabilized (0.2-0.25% Triton X-100 and 10% feral bovine serum or 1 % bovine serum albumin (BSA) in PBS) for 1 hour at room temperature. Next, the cells were

incubated with primary antibodies in 1% BSA in 1X PBS with 0.1% (v/v) Tween 20 (PBST) for 1 hr at room temperature or overnight at 4 °C. Then cells were incubated with the secondary antibodies with fluorophores. For counter-staining of cell nuclei, cells were incubated with 0.1–1 µg/mL Hoechst 34580 (Molecular Probes, Invitrogen, Grand Island, NY) for 1 min. Specific reagents used for different cell types were as follows. *Neurons*: Neuronal class III β -Tubulin (TUJ1) mouse monoclonal antibody (1:500 dilution, Covance Inc., Princeton, NJ) and AlexaFluor-546 goat anti-mouse IgG (1:1000, Invitrogen, Grand Island, NY) were used as the primary and secondary antibodies, respectively^{S12}. *Cardiomyocytes*: Anti- α -actinin mouse monoclonal antibody (1:450; Clone EA-53, Sigma-Aldrich Corp., St. Louis, MO) and AlexaFluor-488 goat anti-mouse (1:200; Molecular Probes, Invitrogen, Grand Island, NY) were used as the primary and secondary antibodies, respectively^{S10}. Hoechst 34580 was used to counter-stain cell nuclei. *HASMC*: Anti-smooth muscle α -actin rabbit polyclonal antibody (1:500, Abcam, Cambridge, MA) and AlexaFluor-488 donkey anti-rabbit antibody (1:200; Molecular Probes, Invitrogen, Grand Island, NY) were used as the primary and secondary antibodies, respectively. Hoechst 34580 was used to counter-stain cell nuclei.

Fluorescent dye labeling of devices and PLGA fibers. Fluorescence images of the reticular nanoES (Fig. 2b and Fig. 3a) were obtained by doping the SU-8 resist solution with rhodamine 6G (Sigma-Aldrich Corp., St. Louis, MO) at a concentration less than 1 µg/mL before deposition and patterning. PLGA electrospun fiber scaffolds were labeled by physical absorption of rhodamine 6G from an aqueous solution (0.1 mg/mL), and then rinsed copiously with water before fluorescence imaging.

Hematoxylin-eosin and Masson trichrome staining. The vascular constructs were cut and fixed in formalin solution (10 %, neutral buffered, Sigma-Aldrich Corp., St. Louis, MO). The fixed sample was dehydrated in a series of graded ethanol baths (70 % ethanol for 1h, 95 % ethanol for 1h, absolute ethanol 3x times, 1h each) and xylenes (2x, 1h each), and then infiltrated with molten paraffin (*HistoStar*, Thermo Scientific, Kalamazoo, MI) at 58 °C for 2h. The infiltrated tissues were embedded into paraffin blocks and cut into 5–6 µm sections. Immediately prior to staining, the paraffin was removed from the sections by 2 washes with xylene, 1 min

each. Then the sections were rehydrated by a 5 min wash in absolute ethanol, 2 min in 95 % ethanol, 2 min in 70 % ethanol and 5 min in distilled water. Standard hematoxylin and eosin staining^{S13} was carried out using an automated slide stainer (Varistain Gemini ES, Thermo Scientific, Kalamazoo, MI). Collagen secretion by HASMCs was assessed on deparaffinized sections using a Masson's trichrome staining kit (Polysciences, Inc., Warrington, PA) according to a standard protocol^{S14}

Optical microscopy and image analysis. Confocal and epi-fluorescence imaging was carried out using an Olympus Fluoview FV1000 confocal laser scanning microscope. Confocal images were acquired using 405, 473 and 559 nm wavelength lasers to excite cellular components labeled with Hoechst 34580, AlexaFluor-488/Rodamine-6G, and Rodamine-6G/AlexaFluor-546 fluorescent dyes (Molecular Probes and Sigma-Aldrich Corp.), respectively. A 635 nm wavelength laser was used for imaging metal interconnects in reflective mode. Epi-fluorescence images were acquired using a mercury lamp together with standard DAPI (EX:377/50,EM:447/60), GFP (EX:473/31,EM520/35) and TRITC (EX:525/40,EM:585/40) filters. *ImageJ* (ver. 1.45i, Wayne Rasband, National Institutes of Health, USA) was used for 3D reconstruction and analysis of the confocal and epi-fluorescence images. Bright-field optical micrographs of histological samples were acquired on an Olympus FSX100 system using FSX-BSW software (ver. 02.02).

Micro-computed tomography. The nanoES in the synthetic vascular construct was imaged using a HMXST Micro-CT x-ray imaging system with a standard horizontal imaging axis cabinet (model:HMXST225, Nikon Metrology, Inc., Brighton, MI). Prior to imaging, samples were fixed and dried. In a typical imaging process, 60-70 kV acceleration voltage and 130-150 μ A electron beam current was used. No filter was used. *VGStudio MAX* (ver. 2.0, Volume Graphics GmbH, Germany) was used for 3D reconstruction and analysis of the micro-CT images.

Cell viability assays. Hippocampal neuron viability was evaluated using a LIVE/DEAD[®] Viability/Cytotoxicity Kit (Molecular Probes, Invitrogen, Grand Island, NY). On days 7, 14 and

21 of the culture, neurons were incubated with 1 μ M calcein-AM and 2 μ M ethidium homodimer-1 (EthD-1) for 45 min at 37 °C to label live and dead cells, respectively^{S9}. Cell viability at each time point was calculated as $\text{live}/(\text{live} + \text{dead}) \times 100$, and been normalized to the percentage of live cells on day 0 ($\text{live}_{\text{day } n}/\text{live}_{\text{day } 0}$). Three-dimensional neuron cultures in MatrigelTM on polylysine modified glass slides (Fisher Scientific Inc., Waltham, MA) were used as controls. The cells were imaged with a confocal fluorescence microscope (Olympus Fluoview FV1000) and the 3D reconstructed images were used for live/dead cell counting. For each group, $n = 6$. In 3D cardiac cultures, cell viability was evaluated with an assay of a mitochondrial metabolic activity, the CellTiter 96® AQueous One Solution Cell Proliferation Assay (Promega Corp., Madison, WI) that uses a tetrazolium compound [3-(4,5-dimethyl-2-yl)-5-(3-carboxymethoxyphenyl)-2-(4-sulfophenyl)-2H-tetrazolium, inner salt; MTS] and an electron coupling reagent (phenazine ethosulfate; PES)^{S15}. On days 2, 4, 6, 8, 10 and 12 of the culture, cardiac constructs were incubated with CellTiter 96® AQueous One Solution for 120 min at 37 °C. The absorbance of the culture medium at 490 nm was immediately recorded with a 96-well plate reader. The quantity of formazan product (converted from tetrazole) as measured by the absorbance at 490nm is directly proportional to cell metabolic activity in culture. Three-dimensional cardiomyocyte cultures in MatrigelTM on gelatin coated electrospun PLGA fibers were used as controls. For each group, $n = 6$.

Electrical measurements. The nanowire FET conductance and transconductance (sensitivity) were measured in $1 \times$ PBS as described previously^{S4}. The slope of a linear fit to conductance versus water-gate potential (V_{gate}) data was used to determine transconductance. For NWFET stability tests, the reticular NWFET devices were maintained under neuron culture conditions (see details above, in **A. Neuron culture**) for predetermined intervals. Electrical transport measurements and recordings from 3D cardiomyocyte-seeded nanoES were obtained in Tyrode solution (pH ~ 7.3) with a 100 mV DC source voltage at 25 °C or 37 °C as described previously^{S4,S16}. The current was amplified with a multi-channel current/voltage preamplifier, filtered with a 3 kHz low pass filter (CyberAmp 380), and digitized at a 50 kHz sampling rate (Axon Digi1440A). In extravascular pH sensing experiments, a single polydimethylsiloxane (PDMS) microfluidic chamber was used to deliver two flows of phosphate buffer solutions: the pH

delivered by the outer input tubing was varied, while that of the inner tubing was fixed at 7.4. In the pH-sensing experiments, nanoelectronic devices were modulated using a lock-in amplifier with a modulation frequency of 79 and 39 Hz, time constant of 30 ms, amplitude of 30 mV, and DC source-drain potential of zero. Ag/AgCl reference electrodes were used in all recording and sensing experiments.

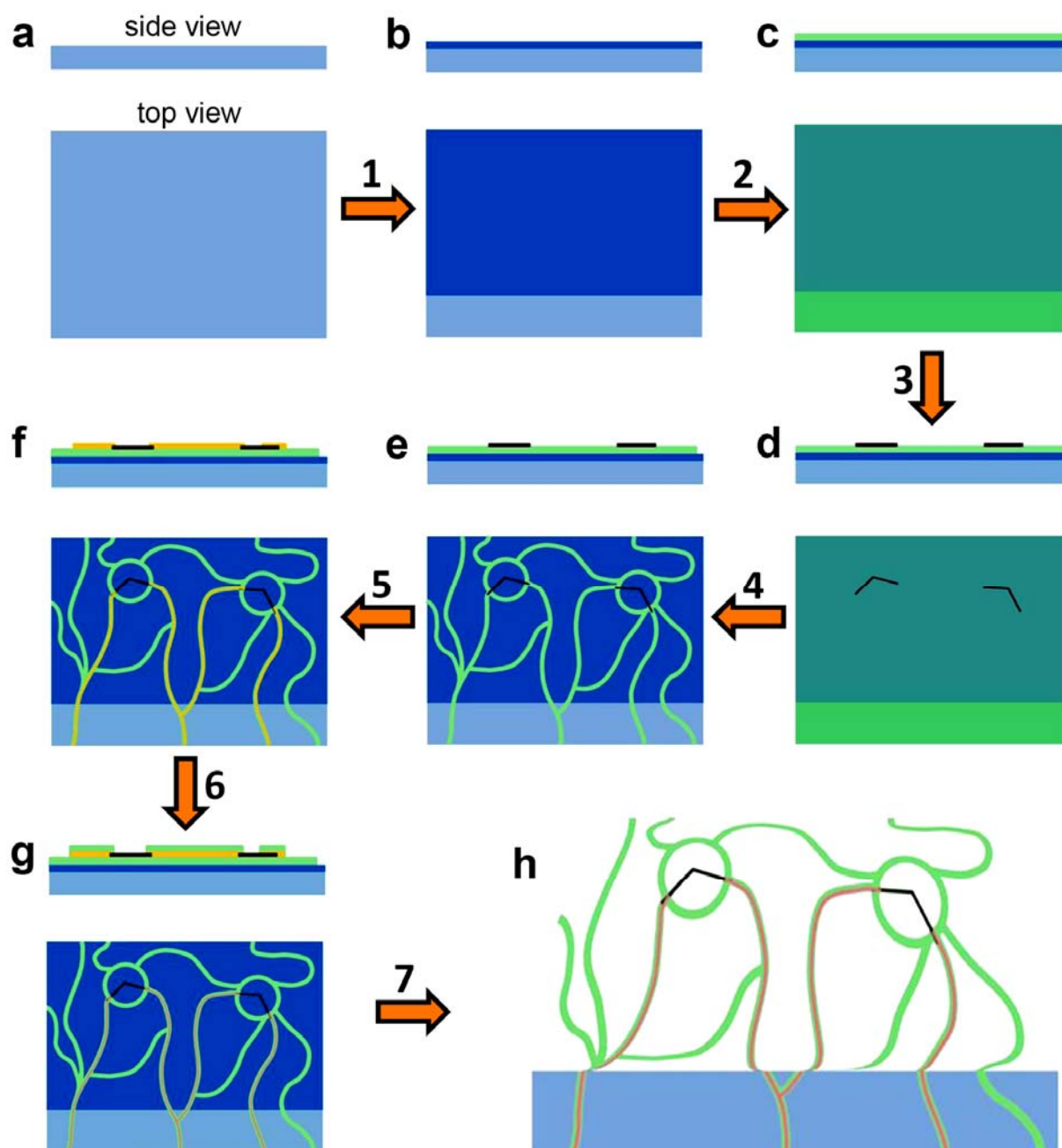


Figure S1 | Schematic of reticular nanoES fabrication. Components include silicon wafer (cyan), nickel relief layer (blue), polymer ribbons (green), metal interconnects (gold) and silicon nanowires (black). In a typical experiment, the widths of polymer and metal interconnects were 1 and 0.7 μm , respectively. The built-in stress from sequentially deposited Cr/Pd/Cr (1.5/50-80/50-80 nm) layers drove self-organization into a 3D scaffold after the lift-off process. Please refer to **Materials and Methods** text for detailed descriptions of steps 1-7.

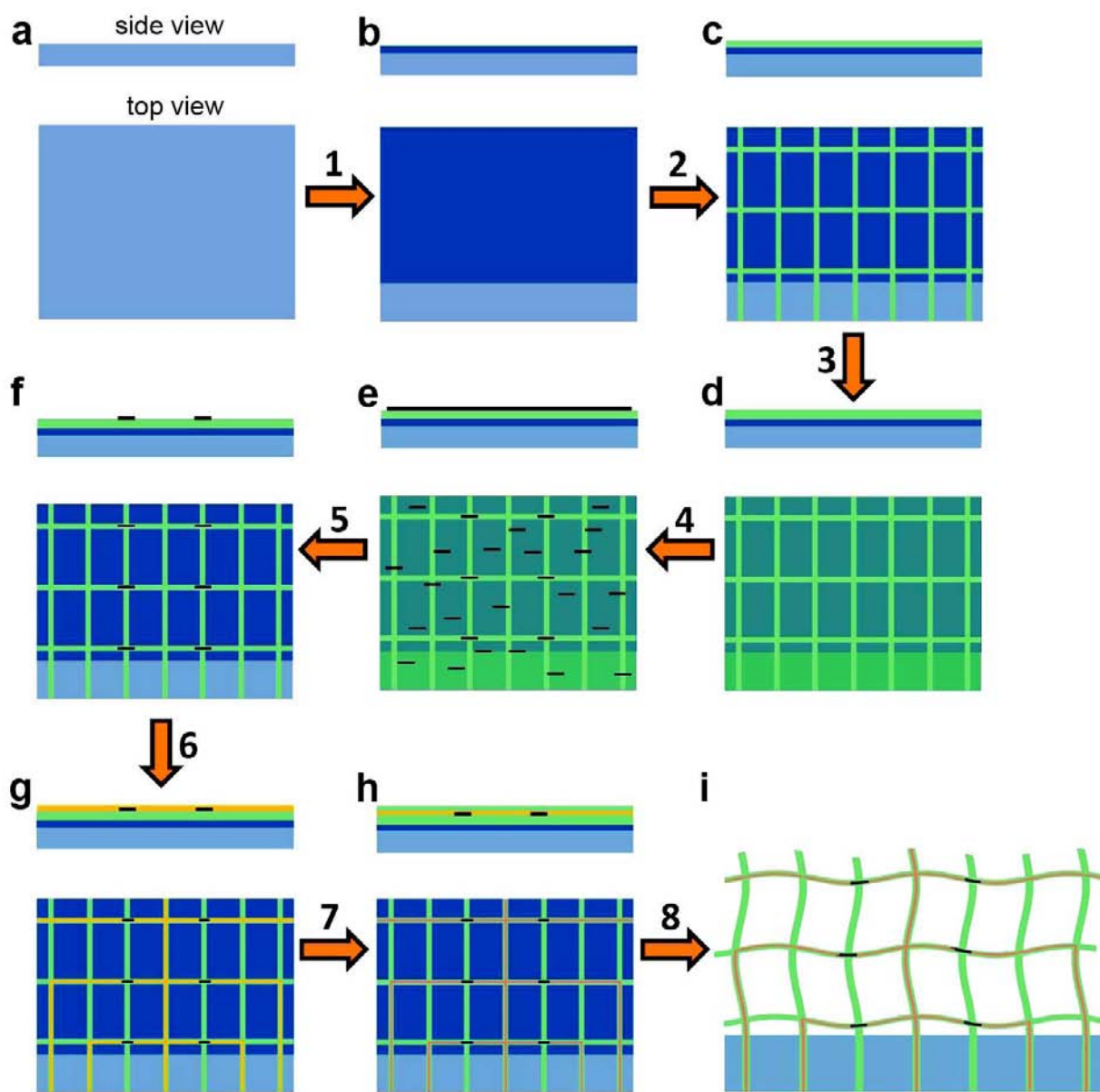


Figure S2 | Schematic of mesh nanoES fabrication. Components include silicon wafer (cyan), nickel relief layer (blue), polymer ribbons (green), metal interconnects (gold) and silicon nanowires (black). The width of the polymer ribbons was 10–40 μm . Symmetrical Cr/Pd/Cr (1.5/50–100/1.5 nm) metals defined by photolithography were used as the minimally stressed nanowire interconnects. 3D device constructs were made by manual folding or rolling of the mesh-like scaffold after (i) (Figs. 2e–2h). Please refer to **Materials and Methods** text for detailed description of steps 1–8.

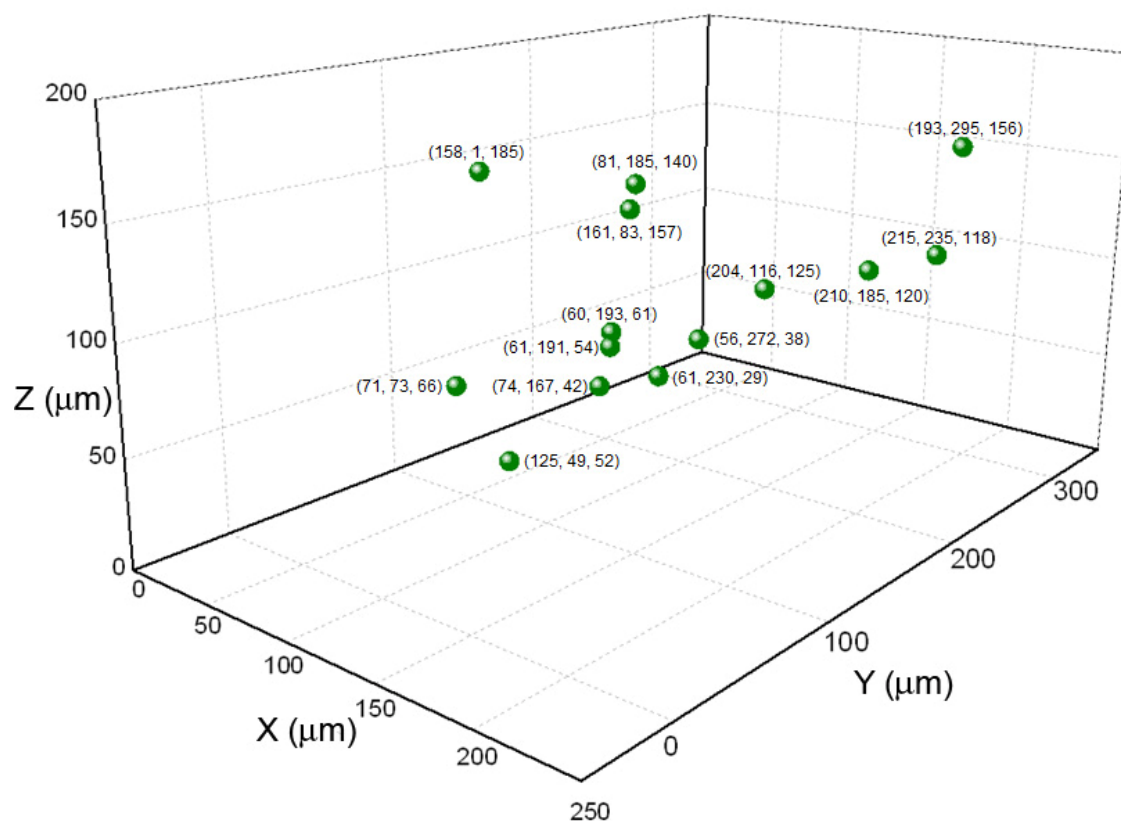


Figure S3 | NWFET 3D distribution in reticular nanoES. 14 NWFETs were distributed in the construct shown in Fig. 2b, II. Individual devices are shown as solid green spheres, with (x, y, z) coordinates in microns denoted for each device point. The overall size of the scaffold, x-y-z was ~ 300-400-200 μm. The NWFET devices within the scaffold were separated in 3D by 7.3 to 324 μm.

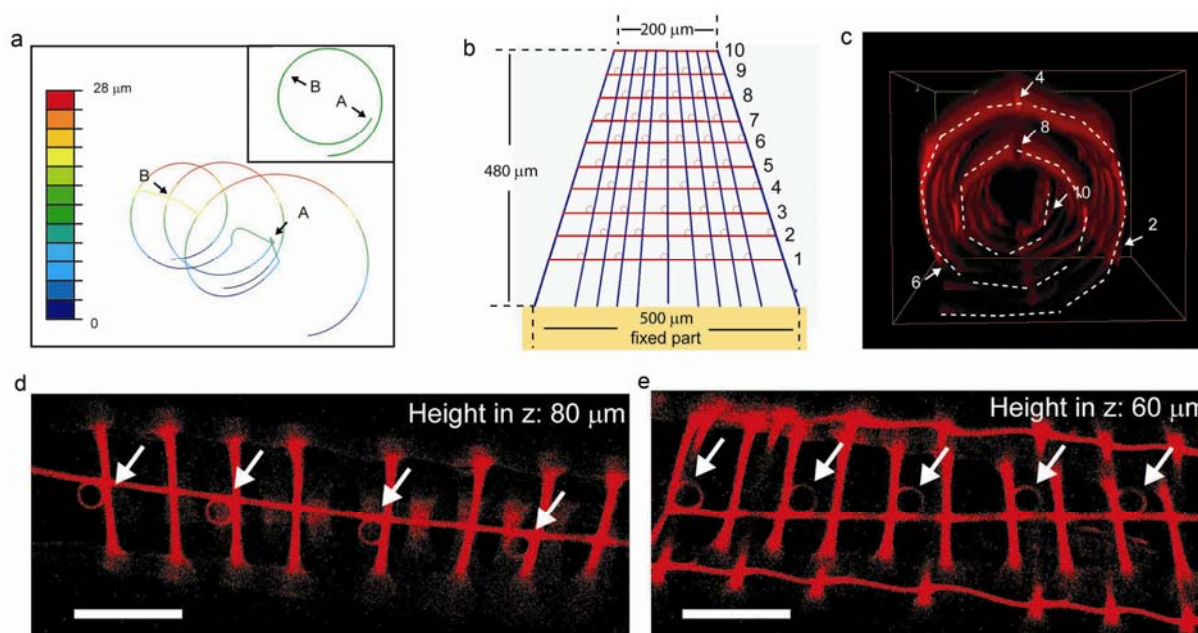


Figure S4 | Design and fabrication of reticular nanoES. (a) Simulation shows that when the equivalent bending moment is increased by 10 times, the subunit structure scrolls up on itself. Inset shows the curve of the central blue ribbon in **Fig. 3a**, demonstrating the devices were scrolled up and different layers were separated. A and B are the two points in **Fig. 3a**. (b-e) Design and fabrication of a much larger and regular matrix, the density of stressed elements increasing upward (from 1 to 10) in a manner analogous to the simulated subunit. (b) The blue lines indicate stressed metal lines with SU-8 as passivation, red lines indicate non-stressed metal lines for interconnection with SU-8 as passivation or SU-8 ribbon as framework, and the circles mark positions for devices. (c) 3D reconstructed confocal fluorescence image shows the side-view of the corresponding fabricated reticular construct following the design in (b). The dashed lines (c) highlight the edge of the 'scrolled-up' reticular nanoES construct. The white numbers and arrows indicate the position of 5 horizontal lines corresponding to those numbered in (b). (d, e) Confocal fluorescence images scanned across the interior of the scaffold at different heights. The images demonstrate that the device regions (circles) are located in planes (heights of 80 and 60 μm are shown) are aligned, and thus demonstrate the regular arrangement in 3D. Scale bars in (d) and (e) are 50 μm . Overall, the results suggest that larger scale simulations could be used to predict the reticular construct geometry, and allow our self-assembling approach to provide regular (or irregular) device arrays distributed through 3D space by design.

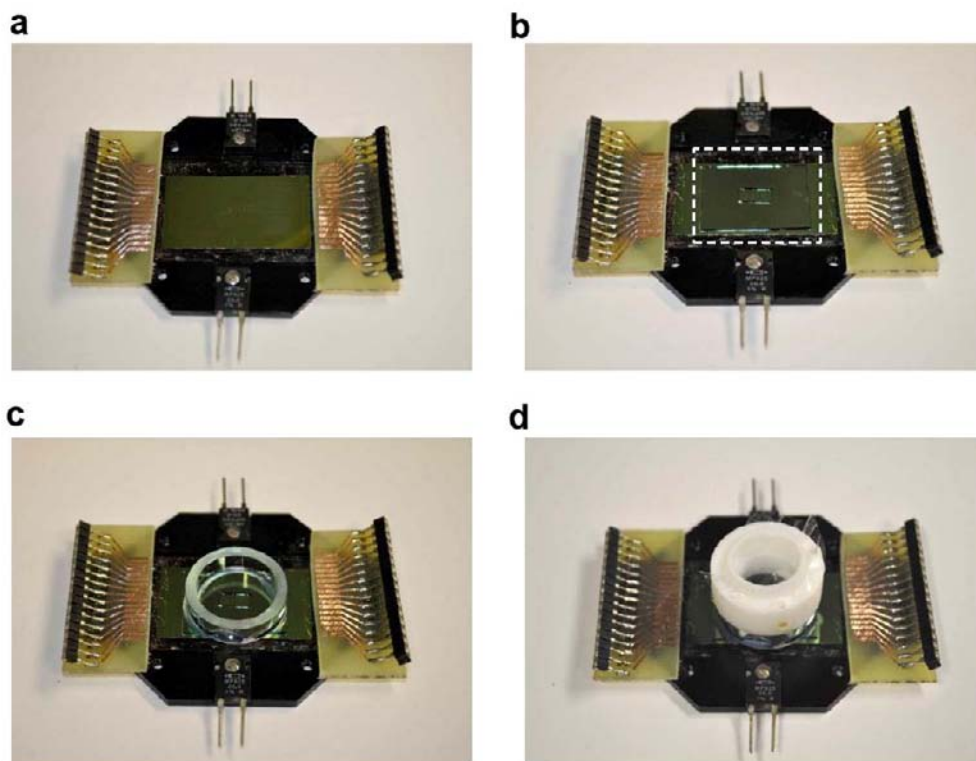


Figure S5 | Chip assembly for neuronal 3D cultures. **a**, A NWFET device chip containing a reticular nanoES was cleaned by O_2 plasma, and assembled onto a temperature controlled chip carrier. **b**, A shallow PDMS chamber (dashed box) was cleaned and placed over the wire-bonded devices. **c**, A glass ring was fixed over the PDMS chamber with silicone elastomer. **d**, A gas-permeable, water-impermeable membrane cover was used for neuron cultures lasting longer than 7 days.

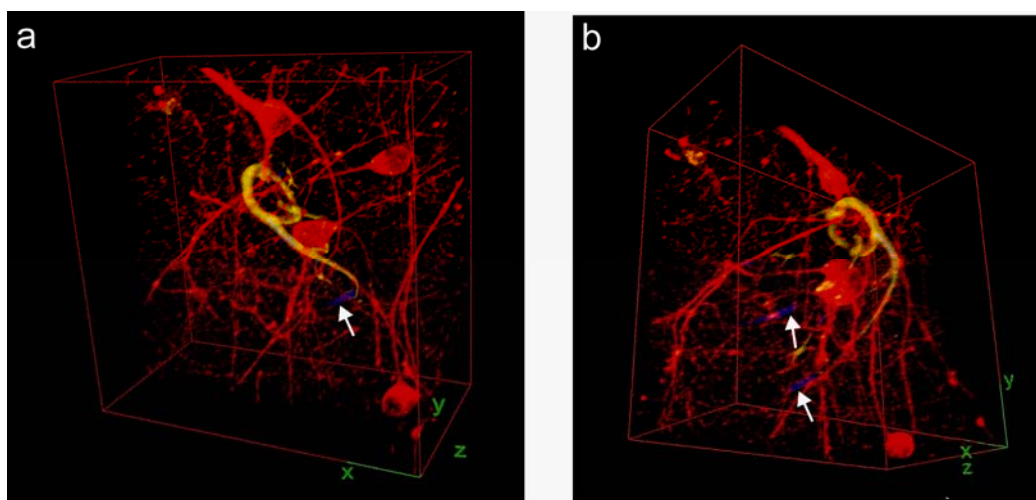


Figure S6 | 3D reconstructed confocal fluorescence image of rat hippocampal neurons within a reticular nanoES. The images show neurons (red, fluorescent antibody against β -Tubulin) and polymer ribbons (yellow, doped with rhodamine 6G dye). The metal interconnects appear as blue, are marked with white arrows, and are imaged in reflected light mode. The images were acquired after two weeks in culture. Dimensions are: x: 127 μm ; y: 127 μm ; z: 68 μm . The images were rotated from the view shown in Fig. 4b approximately as follows: (left image) 90° about z-axis, -10° about y-axis; (right image) 90° about z-axis, 100° about y-axis, 40° about x-axis. Together, these images show unambiguously that neurites pass through the ring-like structures supporting individual nanowire FETs.

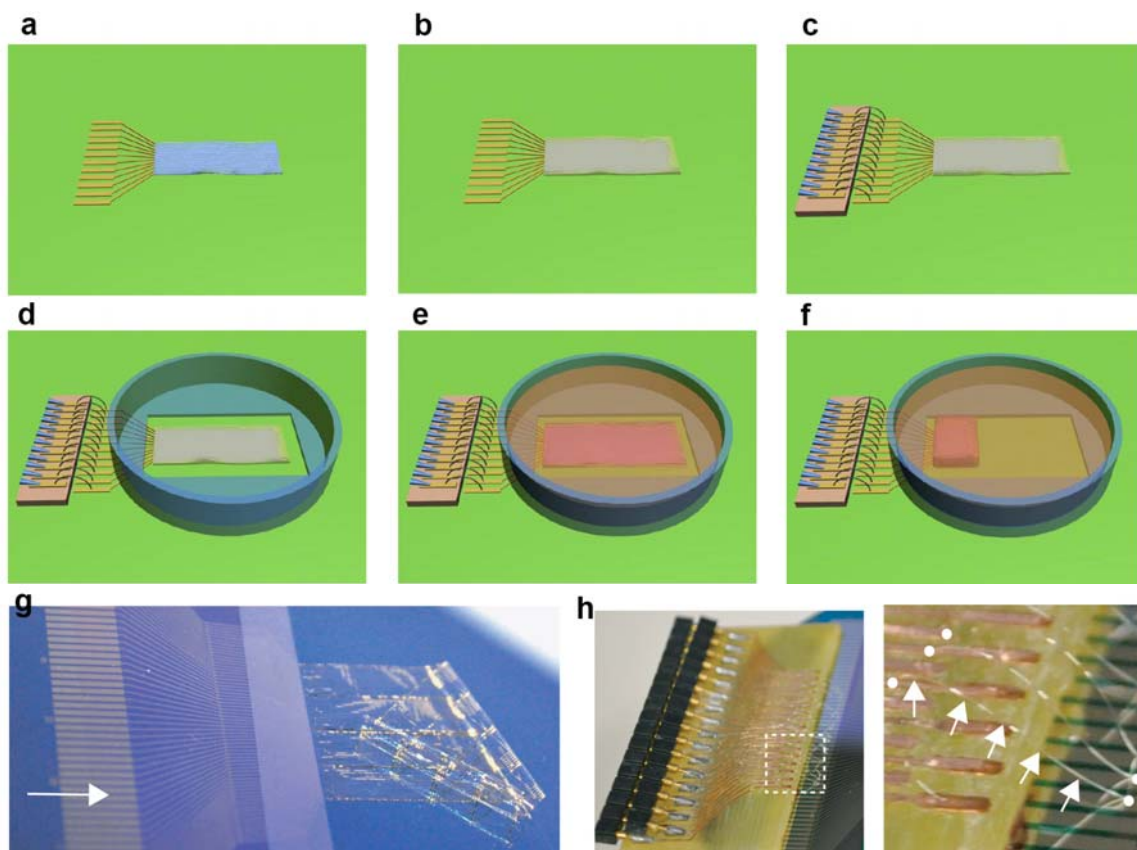


Figure S7 | Schematic of cardiomyocyte 3D culture. **a**, A free-standing mesh-like nanoES. **b**, Hybrid of PLGA electrospun fibers and mesh-like nanoES. **c**, Individual devices were wire-bonded to PCB connectors. **d**, A modified petri-dish was fixed over the scaffold with silicone elastomer. **e**, The hybrid scaffold was sterilized by UV-light illumination for 1 h and soaking in 70 % ethanol solution for 0.5 h, coated with fibronectin/gelatin solution overnight and seeded with cardiomyocytes/Matrigel™. **f**, After 1-2 days in culture, the cardiac sheet (**e**) was folded and cultivated for an additional 3-10 days. **g**, A mesh device showing the free-standing part (the right half) and the fixed part on the wafer (the left half). The arrow marks the outer-electrode pins for wire-bonding. **h**, Printed circuit board (PCB) with wire-bonding wires. The wires connected the PCB copper pads (left) and the rectangular electrodes on the supported end of the mesh-like nanoES (right). White dots highlight bonding points. Arrows highlight one wire-bonded aluminum wire.

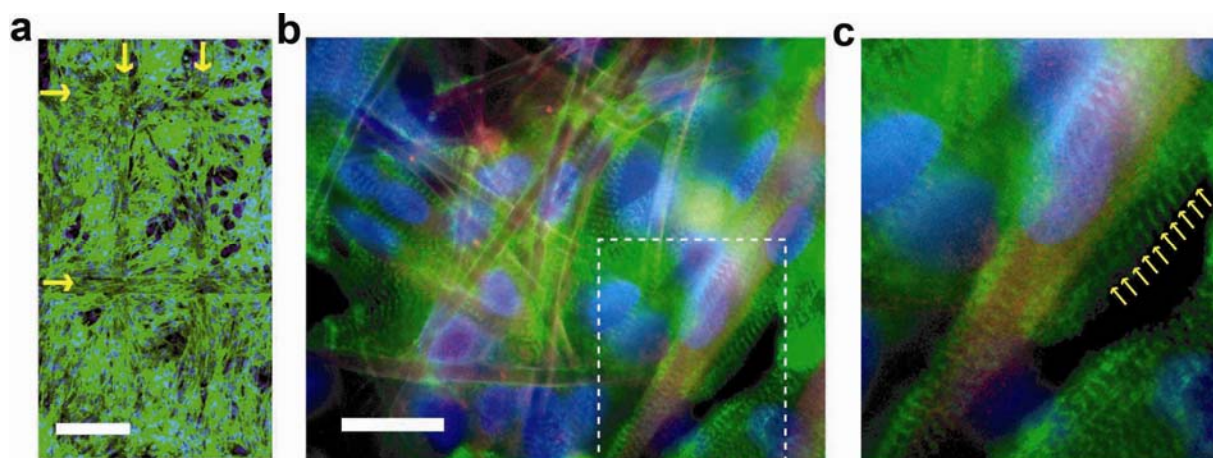


Figure S8 | Fluorescence images from the surface of cardiac cell-seeded nanoES, showing α -actinin of cardiomyocytes (green in **a-c**, Alexa Fluor® 488), cell nuclei (blue in **a-c**, Hoechst 34580) and PLGA fibers (red in **b-c**, rhodamine 6G). Dense cardiomyocyte growth was supported by both nanoES (marked by yellow arrows in **(a)**) and electrospun PLGA fibers in hybrid PLGA/nanoES in **(b)**. **(c)** is a zoomed view of the rectangular box in **(b)**, showing (yellow arrows) striated patterns of α -actinin (green). Scale bars, 200 μm (**a**) and 20 μm (**b**).

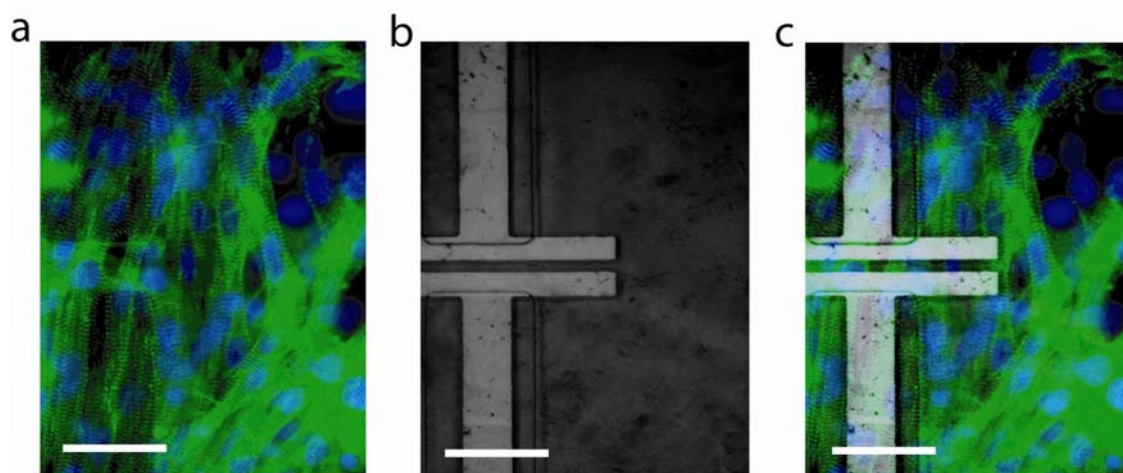


Figure S9 | NanoES – cardiac hybrid tissue. (a) Epi-fluorescence image of the cardiac patch highlighting α -actinin (green, Alexa Fluor® 488) and cell nuclei (blue, Hoechst 34580) of cardiomyocytes. (b) Differential interference contrast (DIC) image of the same sample region, which highlights the S/D electrodes. (c) Overlay of both images to show the positions of S/D electrodes with respect to the cells (right). Scale bars: 40 μ m.

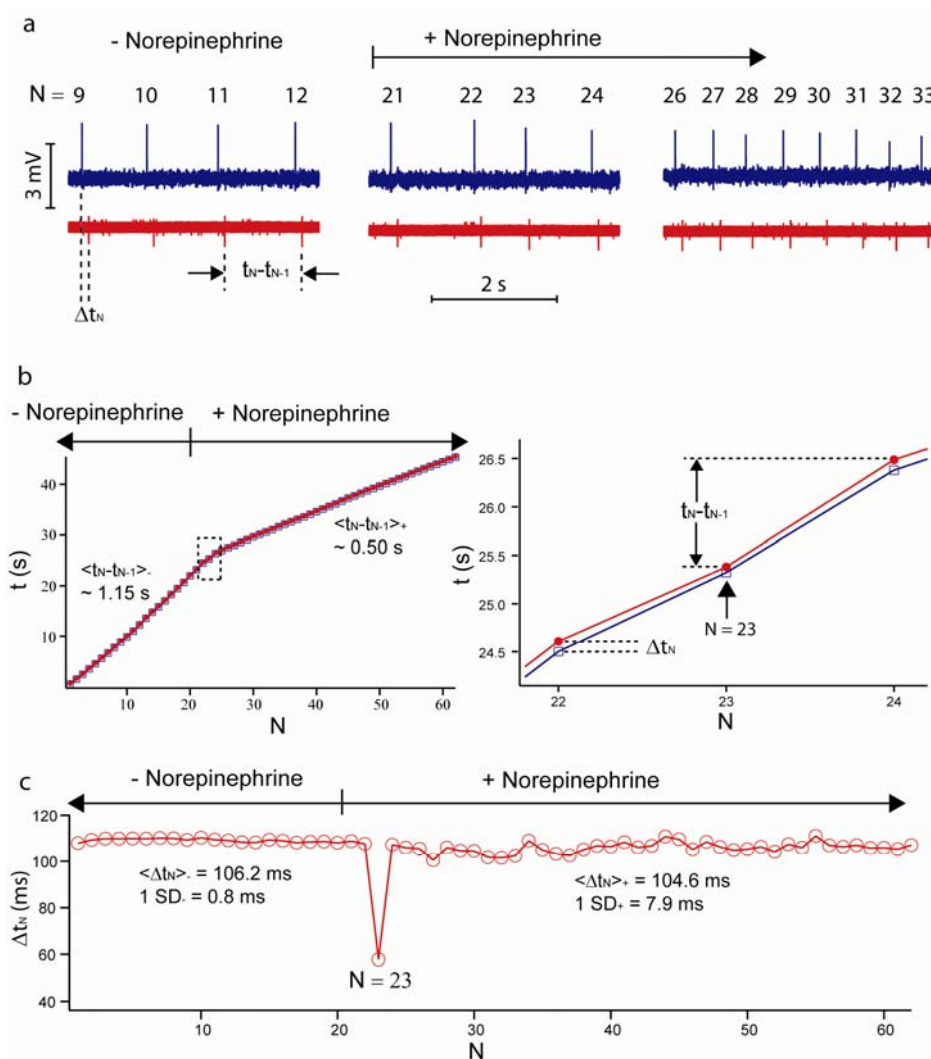


Figure S10 | Multiplexed electrical recording can show cellular heterogeneity in drug response. (a) Electrical recording traces from two devices in a cardiac patch, before (left), during (middle) and after (right) Norepinephrine application. Δt_N is the temporal difference between a pair of spikes from two devices. $t_N - t_{N-1}$ is the interval between consecutive spikes from a single device. N is the spike index. **(b)** The time (t) versus spike index (N) plot, showing a change in slope after norepinephrine application. The slopes correspond to the $\langle t_N - t_{N-1} \rangle$, and are 1.15 s and 0.50 s before and after drug application, respectively. The color coding for devices is the same as in **(a)**. The data show that the cells exhibit overall coherent beating and response to the drug. The right panel is the zoom-in view of the transition, where the middle point ($N=23$) shows a decreased Δt_N compared to earlier and later spikes. **(c)** The Δt_N versus N plot. $\langle \Delta t_N \rangle$ and 1 SD (standard deviation) before (-) and after (+) norepinephrine application show that although the drug has minimum effect on $\langle \Delta t_N \rangle$, the sub-millisecond and millisecond fluctuations of Δt_N (1 SD) increase by ~ 10 fold following drug addition. Such stochastic variation suggests millisecond-level, heterogeneous cellular responses to the drug.

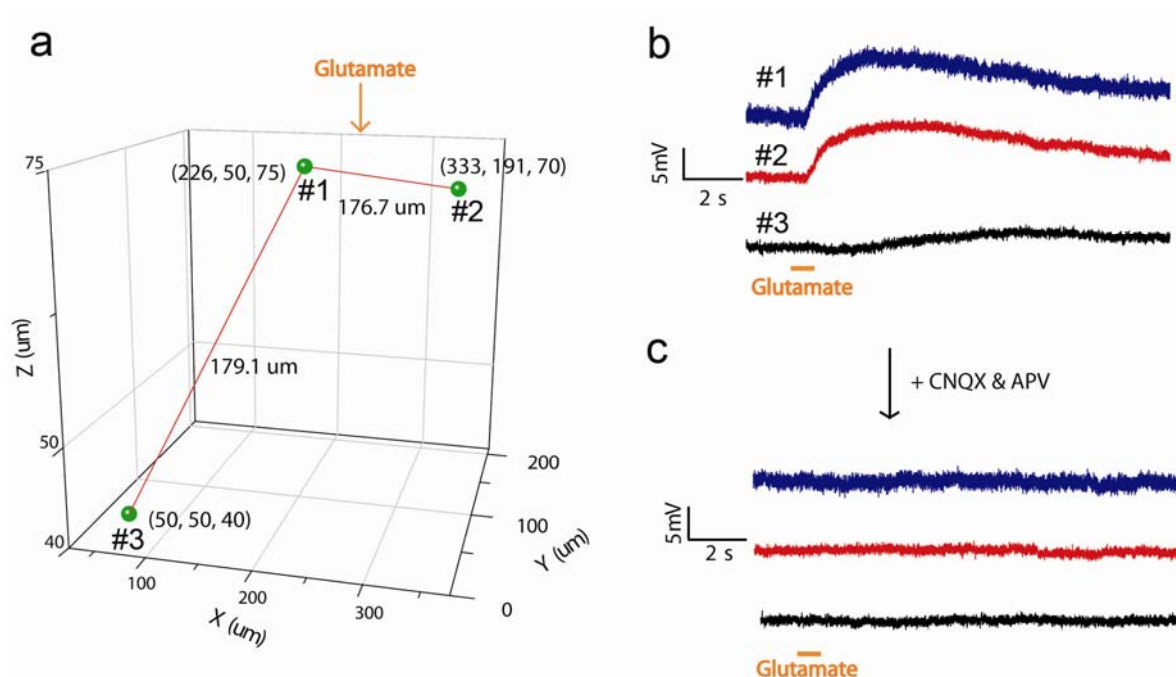


Figure S11, Multiplexed 3D recording from hybrid reticular nanoES/neural constructs. The hybrid nanoES/neural 3D construct was prepared by culturing neurons with a 3D reticular device array for 14 days in vitro with a density of > 4 million neurons/mL in MatrigelTM (Supplementary Information text). During recording, the nanoES/neural hybrid was perfused with an oxygenated artificial CSF (aCSF) containing (in mM) 119 NaCl, 2.5 KCl, 2.5 CaCl₂, 1.3 MgSO₄, 1 NaH₂PO₄, 26.2 NaHCO₃, 22 glucose and equilibrated with 95% O₂/5% CO₂. Three nanowire FETs (labeled **1**, **2** and **3**) were distributed in the construct with x-y-z positions shown in (a). The total sample thickness was ~ 100 μm. The red lines indicate the distances between two devices in 3D. Sodium Glutamate (Sigma) was dissolved in saline solution and further diluted to 20 mM in aCSF solution. Glutamate solution was injected (Micro-injector, Harvard Apparatus) in the middle above device **1** and **2** (orange arrow). The injection pulse duration is 0.5 s. (b) The local field potential changes recorded from three devices in the 3D neuron construct showed distinct position-dependent temporal responses following glutamate solution injection. (c) Perfusing 6-cyano-7-nitroquinoxaline-2,3-dione (CNQX) and D(-)-2-Amino-5-phosphonopentanoic acid (APV) blockers prior to glutamate addition eliminate any observed response, and thus show that the observed response in (b) can be attributed to postsynaptic signal propagation. The orange segments mark the timing when glutamate solution was injected (b and c). The observed responses are consistent with the effects of glutamate, CNQX and APV (Gordon M. Shepherd, *The Synaptic Organization of the Brain*, Oxford University Press, 2004; Jack R. Cooper, *et al. The Biochemical Basis of Neuropharmacology*, Oxford University Press, 2003).

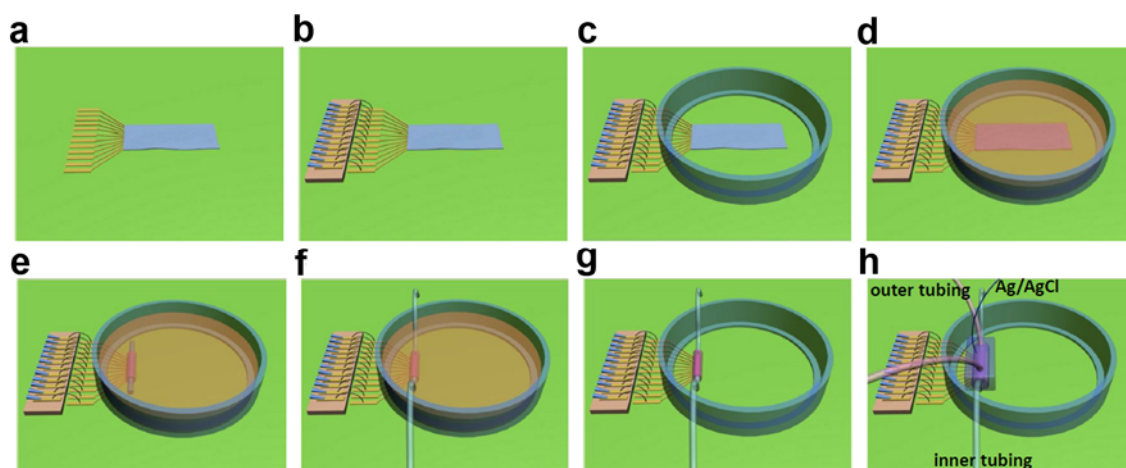


Figure S12 | Schematic of vascular nanoES construct preparation and pH sensing. **a**, A free-standing mesh-like nanoES. **b**, Individual devices were wire-bonded to PCB connectors. **c**, A modified petri-dish was fixed over the scaffold with silicone elastomer. **d**, The hybrid scaffold was sterilized with UV-light illumination for 1 h and soaking in 70 % ethanol solution for 0.5 h, coated with fibronectin/gelatin solution overnight and seeded with HASMCs. **e**, After 7-14 days in culture, the HASMC-seeded nanoES (**d**) was rolled against a tubular support and cultivated for at least another 14 days. **f**, The tubular support was removed and tubing was connected to the ends of the lumen of the HASMC construct. **g**, The medium was removed while keeping the construct moist. **h**, A PDMS chamber was assembled around the construct, attached to tubing to bathe the outside of the construct and Ag/AgCl electrodes to measure pH in the bathing fluid.

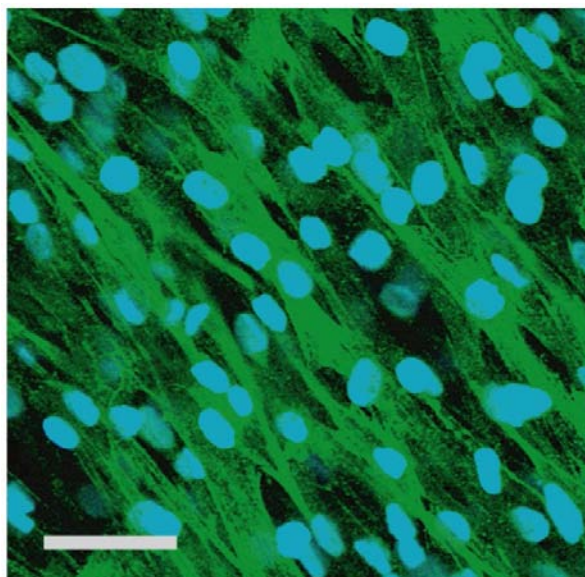


Figure S13 | Confocal fluorescence microscopy image from the surface of the HASMC/mesh-like nanoelectronics biomaterial, showing α -actin (green, Alexa Fluor® 488) and cell nuclei (blue, Hoechst 34580) in smooth muscle cells. Local alignment of HASMCs is revealed by anisotropy in α -actin fibers running from upper left to lower right of image. Scale bars, 40 μ m.

Supplementary References

- S1. Y. Wu, Y. Cui, L. Huynh, C. J. Barrelet, D. C. Bell, C. M. Lieber, Controlled Growth and Structures of Molecular-Scale Silicon Nanowires. *Nano Lett.* **4**, 433-436 (2004).
- S2. C. Yang, Z. Zhong, C. M. Lieber, Encoding Electronic Properties by Synthesis of Axial Modulation Doped Silicon Nanowires. *Science* **310**, 1304-1307 (2005).
- S3. B. Tian, P. Xie, T. J. Kempa, D. C. Bell, C. M. Lieber, Single crystalline kinked semiconductor nanowire superstructures. *Nature Nanotechnol.* **4**, 824-829 (2009).
- S4. B. Tian, T. Cohen-Karni, Q. Qing, X. Duan, P. Xie, C. M. Lieber, Three-dimensional, flexible nanoscale field-effect transistors as localized bioprobes. *Science* **329**, 831-834 (2010).
- S5. D.-H. Kim, *et al.* Epidermal electronics. *Science* **333**, 838-843 (2011).
- S6. K. J. Aviss, J. E. Gough, S. Downes, Aligned electrospun polymer fibres for skeletal muscle regeneration. *Euro. Cells Mater.* **19**, 193-204 (2010).
- S7. S. Timoshenko, S. Woinowsky-Krieger, Theory of Plates and Shells, 2nd edition, P4-6, McGraw-Hill Inc., 1959.
- S8. http://www.genlantis.com/objects/catalog/product/extras/1285_N100200_NeuroPure_E18_Hippocampal_Cells_MV25April2007.pdfS8.
- S9. T. Xu, P. Molnar, C. Gregory, M. Das, T. Boland, J. J. Hickman, Electrophysiological characterization of embryonic hippocampal neurons cultured in a 3D collagen hydrogel. *Biomaterials* **30**, 4377-4383 (2009).
- S10. Y. Sapir, O. Kryukov, S. Cohen, Integration of multiple cell-matrix interactions into alginate scaffolds for promoting cardiac tissue regeneration. *Biomaterials* **32**, 1838-1847 (2011).
- S11. N. L'Heureux, S. Pâquet, R. Labbé, L. Germain, F. A. Auger, A completely biological tissue-engineered human blood vessel. *FASEB J.* **12**, 47-56 (1998).
- S12. S. Pautot, C. Wyart, E. Y. Isacoff, Colloid-guided assembly of oriented 3D neuronal networks. *Nature Methods* **5**, 735-740 (2008).
- S13. J. A. Kiernan, Histological and histochemical methods: theory and practice, 4th edition, Scion publishing Ltd, 2008.
- S14. <http://www.polysciences.com/SiteData/docs/872/4dfadd3f92e8e02f9ac9638745201f1/872.pdf>.
- S15. M. P. Prabhakaran, D. Kai, L. Ghasemi-Mobarakeh, S. Ramakrishna, Electrospun biocomposite nanofibrous patch for cardiac tissue engineering. *Biomed. Mater.* **6**, 055001 (2011).
- S16. T. Cohen-Karni, B. P. Timko, L. E. Weiss, C. M. Lieber, Flexible electrical recording from cells using nanowire transistor arrays. *Proc. Natl. Acad. Sci. USA* **106**, 7309-7313 (2009).